TÜBİTAK

Turkish Journal of Mathematics

http://journals.tubitak.gov.tr/math/

Research Article

Turk J Math
(2015) 39: 23 – 36

doi:10.3906/mat-1312-13

Bifurcation and dynamics of a normal form map

Reza KHOSHSIAR GHAZIANI*
Faculty of Mathematical Sciences, Shahrekord University, Shahrekord, Iran

Received: 10.12.2013 • **Accepted:** 04.06.2014 • **Published Online:** 19.01.2015 • **Printed:** 13.02.2015

Abstract: This paper investigates the dynamics and stability properties of a so-called planar truncated normal form map. This kind of map is widely used in the applied context, especially in normal form coefficients of n-dimensional maps. We determine analytically the border collision bifurcation curves that characterize the dynamic behaviors of the system. We first analyze stability of the fixed points and the existence of local bifurcations. Our analysis shows the presence of a rich variety of local bifurcations, namely stable fixed points, periodic cycles, quasiperiodic cycles that are constraints to stable attractors called invariant closed curves, and chaos, where dynamics of the system change erratically. Our study is based on the numerical continuation method under variation of 1 and 2 parameters and computation of different bifurcation curves of the system and its iterations. For the all codimension 1 and 2 bifurcation points, we compute the corresponding normal form coefficients to reveal the criticality of the corresponding bifurcations as well as to identify different bifurcation curves that emerge around the corresponding bifurcation point. We further perform numerical simulations to characterize qualitatively different dynamical behaviors within each regime of parameter space.

Key words: Normal form coefficients, stable fixed point, chaotic behavior, invariant curve

1. Introduction

Discrete-time dynamical systems generated by iterated maps appear in many scientific areas, such as economics, engineering, and ecology [2, 1, 3, 6, 11, 12, 13, 14, 15, 16, 19, 20]. The usual method for getting an insight into their behavior is to compute many orbits, starting from various initial points (i.e. simulation). Another tool for gaining a better understanding of these systems is bifurcation analysis. It provides theoretic results on the classification of possible modes of behavior, which may explain results of the simulations at different values of control parameters. We consider a 2-dimensional map, introduced in [17], §9.9. This map arises in the normal form of a map near a 1:2 strong resonance point in which the corresponding Jacobian matrix has 2 multipliers, $\mu_{1,2} = -1$. This resonance point serves as an organizing center in bifurcation analysis of an iterated map. There is a smooth invertible change of coordinates, smoothly depending on the parameters, that transforms an n-dimensional map into the planar map [17], Lemma 9.8:

$$\begin{pmatrix} \xi_1 \\ \xi_2 \end{pmatrix} \longmapsto \begin{pmatrix} -1 & 1 \\ \beta_1 & -1+\beta_2 \end{pmatrix} \begin{pmatrix} \xi_1 \\ \xi_2 \end{pmatrix} + \begin{pmatrix} 0 \\ C\xi_1^3 + D\xi_1^2\xi_2 \end{pmatrix} + O(||\epsilon^4||) \tag{1.1}$$

We truncate the map (1.2) to obtain the following map, which has the same asymptotic behavior as (1.1),

$$M : \begin{pmatrix} \xi_1 \\ \xi_2 \end{pmatrix} \longmapsto \begin{pmatrix} -1 & 1 \\ \beta_1 & -1+\beta_2 \end{pmatrix} \begin{pmatrix} \xi_1 \\ \xi_2 \end{pmatrix} + \begin{pmatrix} 0 \\ C\xi_1^3 + D\xi_1^2\xi_2 \end{pmatrix} \tag{1.2}$$

*Correspondence: rkhoshsiar@gmail.com

This map determines the bifurcation scenario of an n-dimensional map near a 1:2 resonance. For more details on parameter-dependent normal form coefficients, we refer to [17] and [18]. In this paper, by means of analytical and numerical tools, we determine all codim-1 and codim-2 bifurcations of the map M. We specially derive an analytical expression for the normal form coefficients of this map for codim-1 bifurcation points. These quantities determine critically the corresponding bifurcation, which shows the direction and stability of the bifurcation point.

The eigenvalues of the Jacobian matrix A of (1.2) are called multipliers. The fixed point is asymptotically stable if $|\mu_i| < 1$ for every multiplier μ_i. If there exists a multiplier μ_i with $|\mu_i| > 1$, then the fixed point is unstable. While following a curve of fixed points, 3 codimension 1 bifurcations can generically occur, namely a limit point (fold, LP) with a multiplier $+1$, a period-doubling point (flip, PD) with a multiplier -1, and a NeimarkSacker point (NS) with a conjugate pair of complex multipliers $e^{\pm\theta i}, 0 < \theta < \pi$. The parameter-dependent normal forms of generic codim-1 bifurcations of fixed points are given in [17]. For fold, flip, and NeimarkSacker, we respectively have

$$w \mapsto w + \beta + aw^2 + O(w^3), \quad w \in \mathbb{R}^1, \tag{1.3}$$

$$w \longmapsto -(1+\beta)w + bw^3 + O(w^4), \quad w \in \mathbb{R}^1, \tag{1.4}$$

$$w \longmapsto we^{i\theta_0}\left(1 + \beta + c|w|^2\right) + O(|w|^4), \quad w \in \mathbb{C}^1, \tag{1.5}$$

where a, b, and $d = \Re(c)$ are the critical normal form coefficients that determine the dynamical behavior near these bifurcation points. The fold bifurcation is nondegenerate if $a \neq 0$. The normal form coefficients b and d are given by:

$$b = \frac{1}{6}\left\langle p, C(q,q,q) + 3B(q,(I-A)^{-1}B(q,q))\right\rangle \tag{1.6}$$

and

$$d = \frac{1}{2}e^{-i\theta_0}\left\langle p, C(q,q,\bar{q}) + 2B(q,h_{11}) + B(\bar{q},h_{20})\right\rangle, \tag{1.7}$$

where

$$h_{11} = (I_n - A)^{-1}B(q,\bar{q}), \quad h_{20} = (e^{2i\theta_0}I_n - A^{-1}B(q,q).$$

For details and proofs we refer to [17], §5.4.2. In the above expressions, A is the Jacobian matrix, and B and C are multilinear forms as follows. Assuming sufficient smoothness of f, we write

$$f(x_0+u,\alpha_0) \;=\; x_0 + Au + B(u,u) + C(u,u,u) \;+ O(\|u\|^4), \tag{1.8}$$

where the components of the multilinear functions B and C are given by

$$B(x,y) \;=\; \sum_{j,k=1}^{n} \frac{\partial^2 f(x_0,\alpha_0)}{\partial\xi_j\partial\xi_k}x_j y_k,$$

$$C(x,y,z) \;=\; \sum_{j,k,l=1}^{n} \frac{\partial^3 f(x_0,\alpha_0)}{\partial\xi_j\partial\xi_k\partial\xi_l}x_j y_k z_l,$$

The flip bifurcation is supercritical, degenerate, or subcritical if b is positive, zero, or negative, respectively. The Neimark–Sacker bifurcation is supercritical, degenerate, or subcritical if d is negative, zero, or positive, respectively.

This paper is organized as follows. In Section 2, we discuss the stability and bifurcation of the fixed points of the map (1.2). We derive analytically the stability regions of fixed points and their bifurcation behaviors. Moreover, we compute analytically the critical normal form coefficients in the case of the period doubling and Neimark–Sacker bifurcations to reveal the criticality of the these bifurcations. Next, in Section 3, we numerically compute curves of fixed points and bifurcation curves of the map and its iterates under variation of 1 and 2 parameters. In this section, we also do numerical simulations to reveal more complex behaviors of the system near a resonance R_4 point. We conclude our work in Section 5 with a discussion of the obtained results.

2. Fixed points of the system and their stability

Bifurcation of maps have been studied intensively in the literature [5, 7, 8, 9]. A comprehensive discussion is given in [17]. We further use the recent results from [10, 18].

We naturally start the bifurcation analysis of (1.2) with the calculation of the fixed points. For all parameter values, this map has the fixed point $E_1 = (0,0)^T$. On the other hand, if (ξ_1, ξ_2) is a nontrivial fixed point, then we have:

$$\begin{aligned} \xi_1 &= -\xi_1 + \xi_2, \\ \xi_2 &= \beta_1\xi_1 + (-1+\beta_1)\xi_2 + C\xi_1^3 + D\xi_1^2\xi_2. \end{aligned} \tag{2.1}$$

From the first equation in (2.1) we obtain:

$$\xi_2 = 2\xi_1. \tag{2.2}$$

The second equation of (2.1) can then be rewritten as:

$$2\xi_1 = \beta_1\xi_1 + 2(-1+\beta_2)\xi_1 + C\xi_1^3 + 2D\xi_1^2\xi_1. \tag{2.3}$$

By (2.2), both components of (ξ_1, ξ_2) must be nonzero. Thus, by dividing both sides of (2.3) by ξ_1 and assuming that $C + 2D \neq 0$, we have:

$$\xi_1^2 = \frac{4 - (\beta_1 + 2\beta_2)}{C + 2D}. \tag{2.4}$$

If

$$\frac{4 - (\beta_1 + 2\beta_2)}{C + 2D} > 0,$$

then 2 further fixed points are $E_2 = (\xi_1, 2\xi_1)$ and $E_3 = (\xi_1, -2\xi_1)$, where

$$\xi_1 = \sqrt{\frac{4 - (\beta_1 + 2\beta_2)}{C + 2D}}.$$

If

$$\frac{4 - (\beta_1 + 2\beta_2)}{C + 2D} = 0,$$

then these points collide with a trivial fixed point. If this happens with β_1 or β_2 as a free parameter in a continuation of trivial fixed points, then clearly we have a pitchfork bifurcation of fixed points.

The Jacobian of (1.2) at a point $(\xi_1, 2\xi_1)$ is given by

$$J(x,y) = \begin{pmatrix} -1 & 1 \\ \beta_1 + 3C\xi_1^2 + 2D\xi_1\xi_2 & -1 + \beta_2 + D\xi_1^2 \end{pmatrix}. \tag{2.5}$$

2.1. Stability and bifurcation of E_1

To derive the stability region in the parameter space, we consider the characteristic equation evaluated in E_1:

$$det(J(E_1) - \lambda I) = det \begin{pmatrix} -1-\lambda & 1 \\ \beta_1 & -1+\beta_2-\lambda \end{pmatrix} = 0, \tag{2.6}$$

i.e.

$$F(\lambda) = \lambda^2 + (2-\beta_2)\lambda + 1 - \beta_1 - \beta_2 = 0. \tag{2.7}$$

To study the stability of E_1 we use Jury's criteria; see [21], §A2.1. Let $F(\lambda) = \lambda^2 - tr(J(E_1))\lambda + det(J(E_1))$ be the characteristic equation of $J(E_1)$. According to Jury's criteria E_1 is asymptotically stable if the following conditions hold:

$$\begin{array}{c} F(-1) = 1 + tr(J(E_1)) + det(J(E_1)) > 0, \\ F(1) = 1 - tr(J(E_1)) + det(J(E_1)) > 0, \\ 1 - det(J(E_1)) > 0. \end{array} \tag{2.8}$$

Applying these conditions leads to

$$\begin{array}{c} F(-1) = \beta_1 < 0, \\ F(1) = \beta_1 + 2\beta_2 < 4, \\ 1 - det(J(E_1)) = \beta_1 + \beta_2 > 0. \end{array} \tag{2.9}$$

Thus, E_1 is asymptotically stable in the parameter region

$$\Omega^S_{E_1} = \{(\beta 1, \beta_2) | \beta_1 + 2\beta_2 < 4, \beta_1 + \beta_2 > 0, \beta_1 < 0\}.$$

The stability boundary of E_1 consists of parts of 3 curves, namely:

1. Curve 1: $\beta_1 + 2\beta_2 = 4$,
2. Curve 2: $\beta_1 + \beta_2 = 0$,
3. Curve 3: $\beta_1 = 0$.

By crossing each of these boundaries, E_1 undergoes a bifurcation. The points of Curve 1 that are on the stability boundary of E_1 satisfy $F(1) = 0$, i.e. they have an eigenvalue $+1$. The points of Curve 2 that are on the stability boundary satisfy $det(J(E_1)) = 1$, i.e. they have 2 eigenvalues with product 1. The points of Curve 3 that are on the stability boundary satisfy $F(-1) = 0$, i.e. they have an eigenvalue -1.

We first note that the product of the 2 multipliers is 1 if and only if $\beta_1 + \beta_2 = 0$, i.e. along Curve 2. In particular, a Neimark–Sacker (NS) point can only be found if $\beta_1 + \beta_2 = 0$. In this case, $\Delta = (2-\beta_2)^2 - 4 = \beta_2(\beta_2 - 4)$. It should be mentioned that Δ is the discriminant of the quadratic polynomial in equation 2.7. Thus, we have true NS points if $\beta_2 \in]0, 4[, \beta_1 = -\beta_2$; we have neutral saddles if $\beta_2 \notin [0, 4], \beta_1 = -\beta_2$.

In particular, we consider the following 3 special cases of the NS bifurcation:

$$\begin{array}{ll} (i) & \beta_1 = -1, \beta_2 = 1, (\theta = \frac{2\pi}{3}) \\ (ii) & \beta_1 = -2, \beta_2 = 2, (\theta = \frac{\pi}{2}) \\ (iii) & \beta_1 = -3, \beta_2 = 3, (\theta = \frac{\pi}{3}) \end{array} \tag{2.10}$$

We note that cases (i) and (ii) are cases with a strong resonance.

It is also easy to see that (2.7) has root -1 if and only if $\beta_1 = 0$, i.e. along Curve 3. The other root then is $-1+\beta_2$.

Along Curve 2, E_1 undergoes a branch point, in which 2 branches of E_2 and E_3 collide to E_1, where $\sqrt{\frac{4-(\beta_1+2\beta_2)}{C+2D}} = 0$.

We will also consider the following case :

$$(iv)\beta_1 = 0, \beta_2 = 1. \tag{2.11}$$

Now consider case (i) in more detail. The characteristic polynomial is:

$$\lambda^2 + \lambda + 1 = 0. \tag{2.12}$$

The eigenvalues of this equation are

$$\lambda_{1,2} = -\frac{1}{2} \pm i\frac{\sqrt{3}}{2}.$$

The normal form coefficient d in this case can be computed explicitly from (1.7) as follows. First we need a right eigenvector $q = (q_1, q_2)^T$ such that

$$\begin{pmatrix} -\frac{1}{2} - i\frac{\sqrt{3}}{2} & 1 \\ -1 & \frac{1}{2} - i\frac{\sqrt{3}}{2} \end{pmatrix} \begin{pmatrix} q_1 \\ q_2 \end{pmatrix} = 0. \tag{2.13}$$

After normalization, we obtain q:

$$\begin{pmatrix} q_1 \\ q_2 \end{pmatrix} = \begin{pmatrix} \frac{1}{\sqrt{2}} \\ \frac{1}{2\sqrt{2}} + i\frac{\sqrt{3}}{2\sqrt{2}} \end{pmatrix}. \tag{2.14}$$

We also need a left eigenvector $p = (p_1, p_2)^T$:

$$\begin{pmatrix} \bar{p}_1 & \bar{p}_2 \end{pmatrix} \begin{pmatrix} -\frac{1}{2} - i\frac{\sqrt{3}}{2} & 1 \\ -1 & \frac{1}{2} - i\frac{\sqrt{3}}{2} \end{pmatrix} = 0. \tag{2.15}$$

Taking into account that $< p, q >= 1$ we get

$$\begin{pmatrix} \bar{p}_1 & \bar{p}_2 \end{pmatrix} = \frac{\sqrt{6}}{6}(\sqrt{3}+i) \begin{pmatrix} 1 & -\frac{1}{2} - i\frac{\sqrt{3}}{2} \end{pmatrix}. \tag{2.16}$$

Now all second-order derivatives of the map M vanish in $(0,0)^{\mathrm{T}}$. Therefore, in (1.7), only the term $C^{(1)}(q, q, \bar{q})$ contributes to the normal form coefficient. We have

$$C^{(1)}(q, q, \bar{q}) = \begin{pmatrix} 0 \\ \sum_{j,k,l=1}^{n} \frac{\partial^3 (C\xi_1^3 + D\xi_1^2\xi_2)}{\partial\xi_j \partial\xi_k \partial\xi_l} q_j q_k \bar{q}_l \end{pmatrix},$$

i.e.

$$C^{(1)}(q, q, \bar{q}) = \begin{pmatrix} 0 \\ 6Cq_1q_1\bar{q}_1 + D(2q_1q_1\bar{q}_2 + 4q_1q_2\bar{q}_1) \end{pmatrix}. \tag{2.17}$$

From $\frac{q_2}{q_1} = \frac{1}{2} + i\frac{\sqrt{3}}{2} = e^{i\frac{\pi}{3}}$, we get

$$q_2 = q_1 e^{i\frac{\pi}{3}}. \tag{2.18}$$

Or, equivalently:

$$\bar{q}_2 = \bar{q}_1 e^{-i\frac{\pi}{3}}.$$

Then we can rewrite (2.17) as follows:

$$C^{(1)}(q,q,\bar{q}) = \begin{pmatrix} 0 \\ 6Cq_1q_1\bar{q}_1 + D[q_1q_1\bar{q}_1(2e^{-i\frac{\pi}{3}} + 4e^{i\frac{\pi}{3}})] \end{pmatrix}. \tag{2.19}$$

Hence,

$$< p, C^{(1)}(q,q,\bar{q}) >= 6C\bar{p}_2q_1q_1\bar{q}_1 + D\bar{p}_2q_1q_1\bar{q}_1(2e^{-i\frac{\pi}{3}} + 4e^{i\frac{\pi}{3}}). \tag{2.20}$$

However, we have

$$\frac{\bar{p}_2}{\bar{p}_1} = -\frac{1}{2} - i\frac{\sqrt{3}}{2} = -e^{i\frac{\pi}{3}}, \tag{2.21}$$

and from $< p, q >= 1$, we have

$$1 = \bar{p_1}q_1 + \bar{p_2}q_2 = -e^{-i\frac{\pi}{3}}\bar{p}_2q_1 + e^{i\frac{\pi}{3}}\bar{p}_2q_1 = (\bar{p}_2q_1)(e^{i\frac{\pi}{3}} - e^{-i\frac{\pi}{3}}), \tag{2.22}$$

so

$$\bar{p}_2q_1 = -\frac{i}{\sqrt{3}}. \tag{2.23}$$

By substituting (2.23) into (2.20), we get:

$$< p, C^{(1)}(q,q,\bar{q}) >= (q_1\bar{q}_1)(-\frac{6i}{\sqrt{3}}C + (1-\sqrt{3}i)D), \tag{2.24}$$

or, equivalently:

$$< p, C^{(1)}(q,q,\bar{q}) >= (q_1\bar{q}_1)(D - i\sqrt{3}(D+2C)). \tag{2.25}$$

Now we define

$$T = \frac{1}{2}e^{-i\theta_0} < p, C^{(1)}(q,q,\bar{q}) >= \frac{1}{2}(q_1\bar{q}_1)(-\frac{1}{2} - i\frac{\sqrt{3}}{2})(D - i\sqrt{3}(D+2C)). \tag{2.26}$$

The real part of T is

$$\frac{1}{2}(q_1\bar{q}_1)(-\frac{1}{2}D - \frac{3}{2}(D+2C)). \tag{2.27}$$

By substituting $q_1\bar{q}_1 = \frac{1}{\sqrt{2}} \times \frac{1}{\sqrt{2}} = \frac{1}{2}$ in the last statement, we obtain:

$$d = -\frac{1}{8}(6C + 4D). \tag{2.28}$$

In the same way, we can analytically obtain the normal form coefficients in the other NS cases. The results are as follows:

- in the case of (ii), i.e. $\theta = \frac{\pi}{2}$: $d = -\frac{1}{12}(6C + 6D)$.

- in the case of (iii), i.e. $\theta = \frac{\pi}{3}$: $d = -\frac{1}{16}(6C + 8D)$.

By similar arguments we obtain in the PD case the normal form coefficient by (1.6), $b = -2C$. Consequently, we have the following theorem.

Theorem 2.1 *The fixed point E_1 is asymptotically stable in $\Omega^S_{E_1}$. Moreover, it loses stability:*

(i) via a Neimark–Sacker along Curve 1. In particular, for $\theta = \frac{2\pi}{3}$, $\theta = \frac{\pi}{2}$, and $\theta = \frac{\pi}{3}$, the associated normal form coefficients are $d = -\frac{1}{8}(6C + 4D)$, $d = -\frac{1}{12}(6C + 6D)$, and $d = -\frac{1}{16}(6C + 8D)$, respectively. In these cases the NS is supercritical (subcritical) if $d > 0$ ($d < 0$).

(ii) via branching along Curve 2, there bifurcating to E_2 and E_3.

(iii) via a flip along Curve 3 with the associated normal form coefficient $b = -2C$, which is supercritical when $C < 0$ and subcritical when $C > 0$.

2.2. Stability and bifurcation of E_2 (E_3)

To determine stability regions of E_2, we again apply Jury's stability criteria. Let $F(\lambda) = \lambda^2 - tr(J(E_2))\lambda + det(J(E_2))$ be the characteristic equation of $J(E_2)$, where

$$tr(J(E_2)) = \frac{-2C + \beta_2(C + 4D) - D\beta_1}{C + 2D}$$

and

$$det(J(E_2)) = -\frac{-11C + 18D + \beta_2(7C + 12D) + \beta_1}{-3C - 2D}.$$

According to Jury's criteria E_2 is asymptotically stable if the following conditions hold:

$$\begin{gathered} F(-1) = \tfrac{-2(6C+8D+\beta_2(3C+4D)+\beta_1(D-C))}{C+2D} > 0, \\ F(1) = -4 - 4\beta_2 + \beta_1 > 0, \\ 1 - det(J(E_2)) = \tfrac{12C+20D+\beta_2(7C+12D)+\beta_1(-3D-2C)}{C+2D} > 0. \end{gathered} \tag{2.29}$$

The stability boundary of E_2 consists of parts of 3 curves, namely:

1. Curve 1: $\beta_1 = 4\beta_2 + 4$, $(F(1) = 0)$,
2. Curve 2: $\beta_1 = \frac{6C+8D+\beta_2(3C+4D}{D+C}$, $(F(-1) = 0)$,
3. Curve 3: $\beta_1 = \frac{12C+20D+\beta_2(7C+12D}{3D+2C}$, $(1 - det(J(E_2)) = 0)$.

By crossing each of these boundaries, E_2 undergoes a bifurcation. Multipliers of $J(E_2)$ along the Curve 1 are:

$$\lambda_1 = 1, \lambda_2 = \frac{-3C - 6D + C\beta_2}{C + 2D}.$$

The multipliers along the Curve 2 are:

$$\lambda_1 = -1, \lambda_2 = \frac{-C - 3D + C\beta_2}{C + D},$$

and the multipliers along the Curve 3 are:

$$\lambda_{1,2} = \frac{-2C + C\beta_2 - 5D \pm \sqrt{(} - 4C^2\beta_2 + 8CD + C^2\beta_2^2 - 10CD\beta_2^2)}{3D + 2C}.$$

Consequently, we have the following theorem.

Theorem 2.2 *The fixed point E_2 is asymptotically stable if the conditions of (2.29) hold. Moreover, it loses stability:*

(i) via a branch point along Curve 1, there bifurcating to E_1.

(ii) via a flip point along Curve 2.

(iii) via a Neimark–Sacker point along Curve 3 provided that $-4C^2\beta_2 + 8CD + C^2\beta_2^2 - 10CD\beta_2^2 < 0$.

3. Numerical stability and bifurcation of the map M

Numerical bifurcation analysis reveals more complicated dynamics of the map and its iterates. The theoretically computed values can also be checked numerically when continuing the fixed point curve. The bifurcation analysis is based on continuation and bifurcation methods for maps, tracing out the solution manifolds of fixed points while some of the parameters of the map vary. See [4, 10].

3.1. Numerical bifurcation of E_1

First we continue the fixed point curve numerically to detect the NS point in case (i). To do numerical continuation we fix the parameter values $\beta_1 = -1$, $C = D = 1$ and continue E_1 with the free parameter β_2. We see that the fixed point E_1 is stable when $1 < \beta_2 < 2.5$. It loses stability via a supercritical NS point when $\beta_2 = 1$, and via a branch point when β_2 crosses 2.5. These results are consistent with Theorem 2.1 since $(\beta_1, \beta_2) \in \Omega^S_{E_1}$ for all $\beta_2 \in]1, 2.5[$. The numerical results, Run 1, are given below.

```
label = NS   , x = ( 0.000000 0.000000 1.000000 )
 normal form coefficient of NS = -1.250000e+000
label = BP   , x = ( 0.000000 0.000000 2.500000 )
```

The first 2 entries of x are the coordinate values of the fixed point E_1, and the last entry of x is the value of the free parameter β_2 at the corresponding bifurcation point. We note that the normal form coefficient of the NS point is -1.25, confirming Theorem 2.1, part (i), where $d = -\frac{1}{8}(6C + 4D) = -1.25$ for $C = D = 1$.

We also compute numerically a branch point (BP) for $\beta_2 = 2.5$. By (2.4) the nontrivial fixed points collide to a trivial fixed point when

$$4 - (\beta_1 + 2\beta_2) = 0. \tag{3.1}$$

The fixed parameter is $\beta_1 = -1$, and this implies that in a BP $\beta_2 = 2.5$ in (3.1). This confirms the numerical result concerning the BP point.

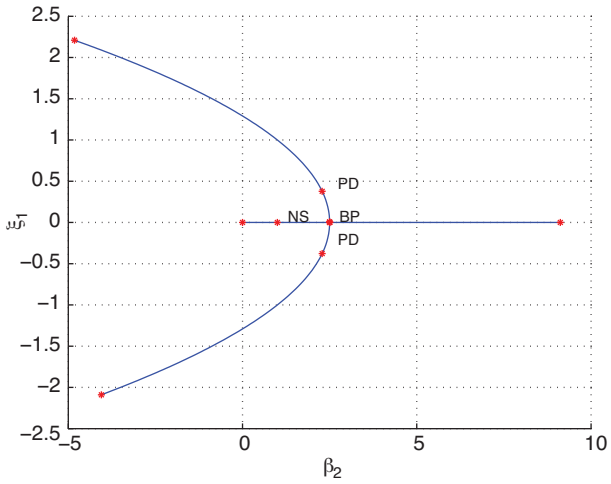

Figure 1. Continuation of trivial and nontrivial fixed points of the map M in (β_2, ξ_1) space.

The Jacobian is given by:

$$[M_x - I|M_{\beta_2}] = \begin{pmatrix} -2 & 1 & 0 \\ \beta_1 & -2+\beta_2 & 0 \end{pmatrix}. \tag{3.2}$$

If $\beta_1 = -1$ and $\beta_2 = 2.5$, then this reduces to:

$$[M_x - I|M_{\beta_2}] = \begin{pmatrix} -2 & 1 & 0 \\ -1 & 0.5 & 0 \end{pmatrix}. \tag{3.3}$$

Clearly $[M_x - I|M_{\beta_2}]$ is rank deficient as expected.

Now we compute the new branch in the BP point. The new branch is a set of nontrivial fixed points that are a parabola in (β_2, ξ_1) space. A picture of the continued trivial fixed point in Run 1 and the computed nontrivial fixed points are presented in Figure 1.

3.2. Numerical bifurcation of E_2 (E_3)

We now consider $E_2 = (0.860916, 1.721832)$, which is in the stable region for the parameter values $\beta_1 = 0.3, \beta_2 = 5, C = -2.5$, and $D = -3$ (stability follows from Theorem 2.2). We do a numerical continuation of E_2 with control parameter β_2. The output, Run 2, is given by:

```
label = NS   , x = ( 0.343232 0.686464 2.350685 )
 normal form coefficient of NS = -2.114932e+001
label = PD   , x = ( 0.124035 0.248069 1.915385 )
 normal form coefficient of PD = -1.523118e+001
label = BP   , x = ( -0.000000 -0.000000 1.850000 )
```

E_2 is stable when $1.915385 < \beta_2 < 2.350685$. It loses stability via a supercritical Neimark–Sacker point when $\beta_2 = 2.350685$, which is consistent with Theorem 2.2, part (iii). It also loses stability through a subcritical PD point when $\beta_2 = 1.915385$, which is consistent with Theorem 2.2, part (iii).

The dynamics of the system prior to the PD point consists of an unstable 2-cycle that coexists with a stable fixed point. Beyond the NS point the dynamics of the system consists of a stable closed invariant that coexists with unstable fixed points of the map M. For $\beta_2 = 2.3510$ a stable closed invariant curve is created around the unstable fixed point E_2 (see Figure 2).

Now we compute the period doubling curve, with β_2 and C free, by starting from the PD point of Run 2. We call this Run 3.

```
label = R2   , x = ( 0.974679 1.949359 2.850000 3.894737 )
Normal form coefficient for R2 :[c , d]= 1.216842e+001, -2.684210e+001
```

This computed PD curve is shown in Figure 3 (lower curve). Now we compute the NS curve, with β_2 and C free parameters, by starting from the NS point of Run 2. We call this Run 4.

```
label = R3   , x = ( 0.730297 1.460594 2.600000 3.187500 -0.500000 )
Normal form coefficient of R3 : Re(c_1) = -3.642213e-001
label = R2   , x = ( 0.974679 1.949359 2.850000 3.894737 -1.000000 )
Normal form coefficient of R2 : [c , d] = 1.215940e+001, -2.682222e+001
label = R4   , x = ( 0.341565 0.683130 2.350000 -2.571429 0.000000 )
Normal form coefficient of R4 : A = -3.719269e+000 + -4.521757e-001 i
```

The computed curve of NS points is also shown in Figure 3 (upper curve).

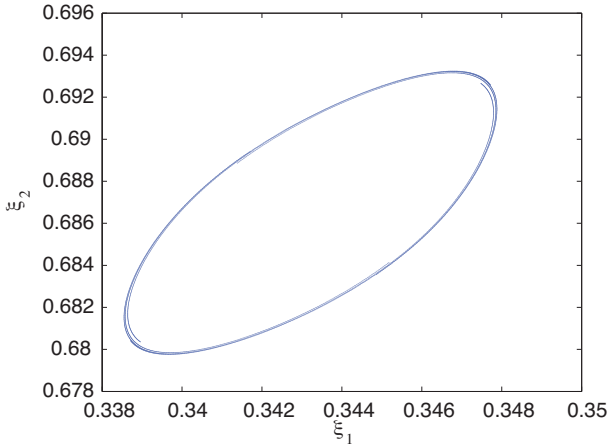

Figure 2. A limit cycle for $\beta_1 = 0.3, \beta_2 = 2.3510, C = -2.5$, and $D = -3$.

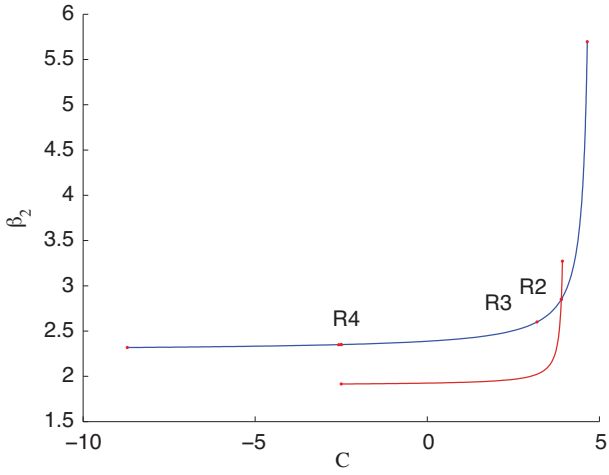

Figure 3. Flip and Neimark–Sacker bifurcation curves starting from points in Run 2.

The normal form coefficient A of the R4 point in Run 4 satisfies $|A| > 1$, and hence 2 cycles of period 4 of the map are born. A stable 4-cycle for $\beta_1 = 0.3, \beta_2 = 2.419620924343121, C = -3.219952966567809$, and $D = -3$ is given by: C4 = X1, X2, X3, X4 where X1 = (0.313943351106174, 0.545162737134870). In order to compute the stability region of this 4-cycle, we compute 2 fold curves of the fourth iterate rooted at the R4 point. These curves exist since $|A| > 1$; see [17]. We can thus switch from the R4 point to the fold curves of the fourth iterate. The stable fixed points of the fourth iterate exist in the wedge between the 2 fold curves (LP^4 curves) and a flip curve of the fourth iterate (PD^4 curve). The computed LP^4 curves and PD^4 curve are shown in Figure 4.

We further compute a curve of fixed points of the fourth iterate starting from the 4-cycle C_4 with control parameter C. The curve is presented in Figure 5.

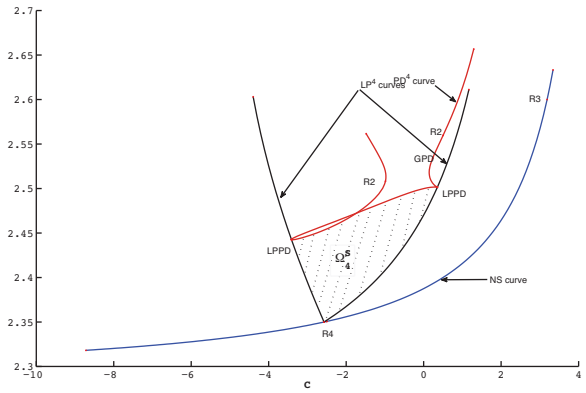

Figure 4. NS bifurcation curve, 2 branches of LP^4 cycles rooted at the $R4$ point, and a PD^4 curve rooted at the $LPPD$ point. These curves form stability boundaries of 4-cycles Ω_4^S.

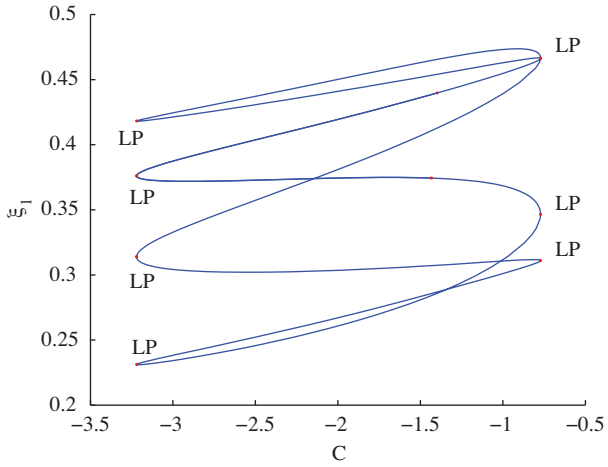

Figure 5. Curve of fixed points of the fourth iterate starting from the 4-cycle C_4.

4. Numerical simulation

To reveal the qualitative dynamical behaviors of (1.2) near the computed NS point corresponding to $\beta_2 = 1$, in Run 1, we present a complete bifurcation sequence that is observed for different values of $\beta_2 = 1$. We fix the parameters $\beta_1 = -1, C = 1, D = 1$ and consider several values of β_2.

Figure 6 shows that E_1 is a stable attractor for $\beta_2 = 1.01$. The behavior of (1.2) before the NS point at $\beta_2 = 1.002$ is depicted in Figure 7.

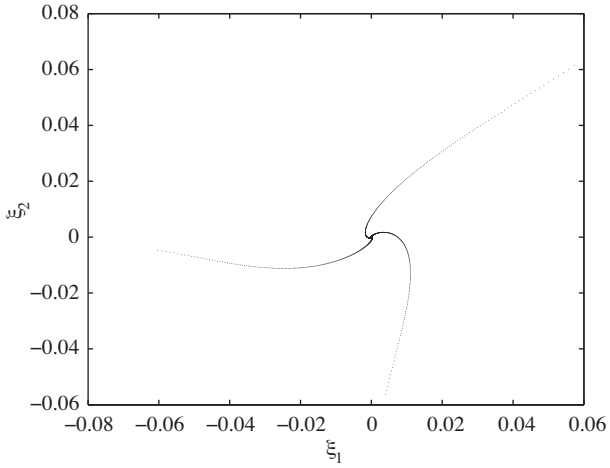

Figure 6. An attracting fixed point for system (1.1) that exists for $\beta_2 = 1.01$.

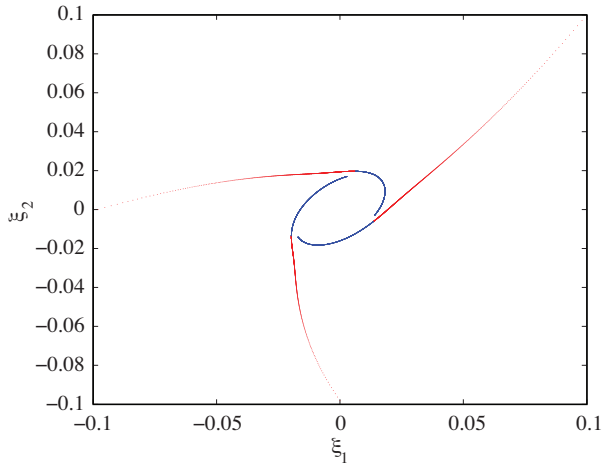

Figure 7. Phase portrait for the system (1.2) that exists for $\beta_2 = 1.002$.

Figure 8 demonstrates the behavior of the model after the NS bifurcation when $\beta 2 = 0.9$. From Figure 7 and Figure 8 it turns out that the fixed point F_3 loses its stability through a NS bifurcation when β_2 varies from 0.9 to 1.01. Since the critical normal form coefficient corresponding to the NS point is negative, then a stable closed invariant curve bifurcates from E_1, which coexists with unstable fixed point E_1. Figure 8 demonstrates and confirms the above statement.

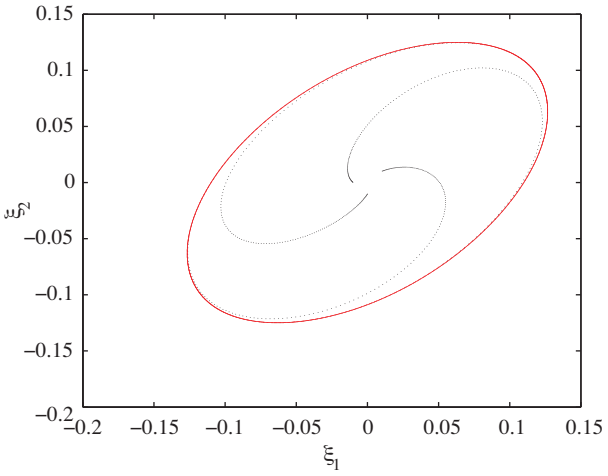

Figure 8. A phase portrait for the system (1.2) for $\beta_2 = 0.9$.

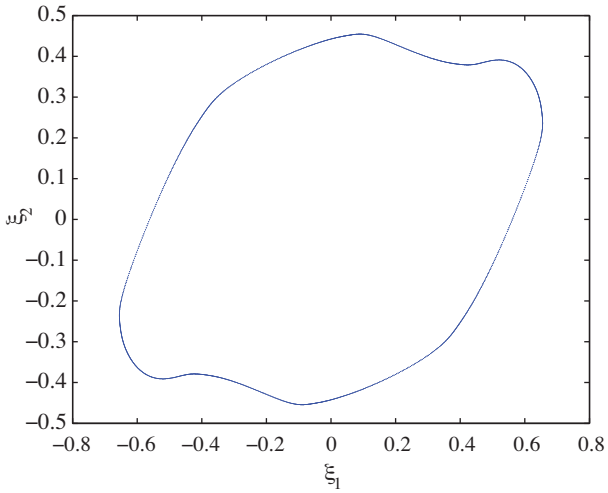

Figure 9. The breakdown of the closed invariant curve of the system (1.2) for $\beta_2 = 0.55$.

As β_2 is increased further, however, the phase portrait starts to fold. We see that the circle, after being stretched, is shrunken and folded, creating new phenomena due to the breakdown of the closed curve; see Figure 9. For further increasing β_2 we obtain the multiple invariant closed curves brought about by the NS bifurcation point of iterates of (1.2). In these cases higher bifurcations of the torus occur as the system moves out of the quasiperiodic region by increasing β_2. The dynamics move from one closed curve to another periodically, but the dynamics in each closed curve may be periodic or quasiperiodic. Figure 10 presents the set of closed curves around the NS bifurcation. Figure 11 presents a strange attractor for $\beta_2 = 0.45$ that exhibits fractal structure.

5. Concluding remarks

We investigated the dynamical behavior of a discrete map arising in normal form of a map near a 1:2 strong resonance point. In Section 2, we focused on the stability and possible bifurcations of 3 types of fixed points of the map denoted by E_1, E_2, and E_3. We established the stability condition and branching behavior of E_1, and conditions under which E_1 may bifurcate to a NeimarkSacker, flip, or branch point were derived in Theorem 2.1. We also proved the criticality of the flip and Neimark–Sacker bifurcations of E_1 by computing analytically the corresponding normal form coefficients. In Section 3, we computed curves of fixed points and bifurcation curves of several iterates. In particular, we computed the parameter region of stability of the 4-cycle (Ω_4^4) surrounded by the flip bifurcation curve of the fourth iterate (PD^4) and 2 branches of fold bifurcations of the fourth iterate (LP^4). By branch switching, we also computed a secondary branch of fixed points of E_2 emanating from a branch point on a curve of fixed points of E_1. We further used a numerical simulation method to reveal chaotic behaviors and a strange attractor near the Neimark–Sacker bifurcation.

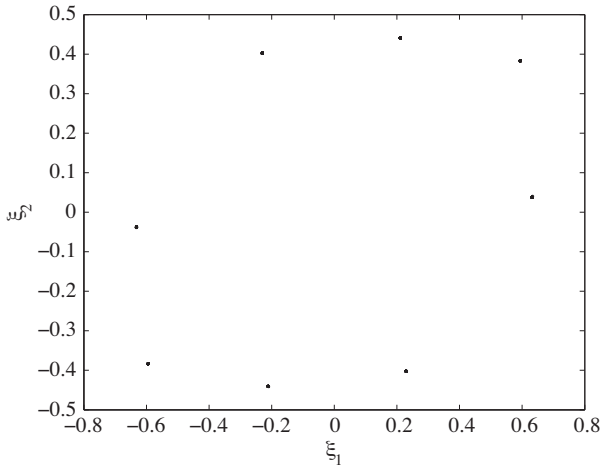

Figure 10. The existence of multiple closed curves of the system (1.2) for $\beta_2 = 0.45$.

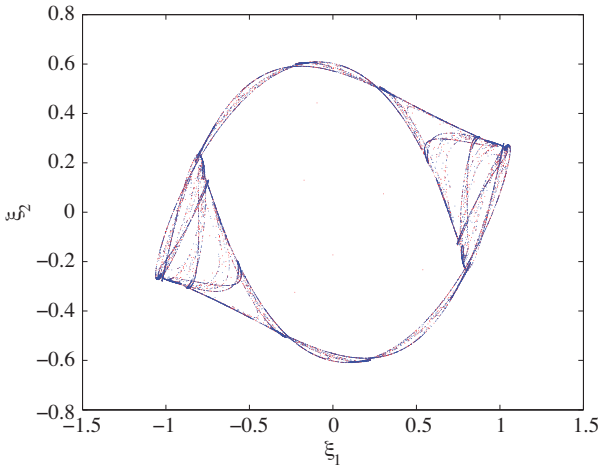

Figure 11. Chaotic attractor for the system (1.2) that exists for $\beta_2 = 0.45$.

Acknowledgments

The author would like to thank Shahrekod University for the financial support of this work through a research grant. The author was also partially supported by the Center of Excellence for Mathematics, Shahrekord University.

References

[1] Agiza HN, Bischi GI, Kopel M. Multistability in a dynamic Cournot game with three oligopolists. Math Comput Simult 1999; 51: 63–90.

[2] Agiza HN, Elabbasy EM, El-Metwally H, Elsadany A. Chaotic dynamics of a discrete preypredator model with Holling type II. Nonlinear Anal Real 2009; 10: 116–129.

[3] Agiza HN, Elsadany A, Kopel M. Nonlinear dynamics in the Cournot duopoly game with heterogeneous players. Physica A 2003; 320: 512–524.

[4] Allgower EL, Georg K. Numerical Continuation Methods: An Introduction. New York, NY, USA: Springer-Verlag, 1990.

[5] Beddington JR, Free CA, Lawton J. H. Dynamic complexity in predator-prey models framed in difference equations. Nature 1975; 255: 58–60.

[6] Bischi GI, Mammana A, Gardini L. Multistability and cyclic attractors in duopoly games. Chaos Soliton Fract 2000; 11: 543–564.

[7] Carcasss JP. Determination of different configurations of fold and flip bifurcation curves of one or two-dimensional map. Int J Bifurcat Chaos 1993; 4: 869–902.

[8] Carcasss JP. Singularities of the parametric plane of an n-dimensional map. Determination of different configurations of fold and flip bifurcation curves. Int J Bifurcat Chaos 1995; 5: 419–447.

[9] Carcasss JP, Mira C, Sim C, Bosch M, Tatjer JC. Cross-road areaspring area transition. I: Parameter plane representation. Int J Bifurcat Chaos 1991; 2: 339–348.

[10] Govaerts W, Khoshsiar Ghaziani R, Kuznetsov Y, Meijer HG. Numerical methods for two-parameter local bifurcation analysis of maps. Siam J Sci Comput 2007; 29: 2644–2667.

[11] Guckenheimer J, Holmes P. Nonlinear Oscillations, Dynamical Systems, and Bifurcations of Vector Fields. New York, NY, USA: Springer-Verlag, 1985.

[12] He Z, Lai X. Bifurcation and chaotic behavior of a discrete-time predatorprey system. Nonlinear Anal Real 2011; 12: 403–417.

[13] Holling CS. The functional response of predator to prey density and its role in mimicry and population regulation. Mem Entomol Soc Can 1965; 45: 1–60.

[14] Jiao J, Meng XZ. Global attractivity and permanence of a stage-structured pest management SI model with time delay and diseased pest impulsive transmission. Chaos Soliton Fract 2008; 38: 658–668.

[15] Jing Z, Yang J. Bifurcation and chaos in discrete-time predator-prey system. Chaos Soliton Fract 2006; 27: 259–277.

[16] Kraft RL. Chaos, Cantor sets, and hyperbolicity for the logistic maps. Am Math Mon 1999; 106: 400–408.

[17] Kuznetsov Y. Elements of Applied Bifurcation Theory. 3rd ed. New York, NY, USA: Springer-Verlag, 2004.

[18] Kuznetsov Y, Meijer HG. Numerical normal forms for codim 2 bifurcations of maps with at most two critical eigenvalues. Siam J Sci Comput 2005; 26: 1932–1954.

[19] Kuznetsov Y, Meijer HG. Remarks on interacting Neimark-Sacker bifurcations. J Differ Equ App 2006; 12: 1009–1035.

[20] Lauwerier HA. Two-dimensional iterative maps. Chaos Nonlinear Sci Theory Appl 1986; 32: 58–95.

[21] Murray JD. Mathematical Biology. 2nd ed. Berlin, Germany: Springer, 1993.